Cluster structure and γ transitions in actinide nuclei

B. Buck and A. C. Merchant
Department of Physics, University of Oxford, Theoretical Physics, 1 Keble Road, Oxford OX1 3NP, United Kingdom

S. M. Perez
Department of Physics, University of Cape Town, Private Bag, Rondebosch 7700, South Africa

(Received 30 July 1998)

We summarize the recent accumulation of data on electromagnetic transitions between states belonging to the lowest positive and negative parity bands of nuclei in the actinide region, and show that, in the case of $E2$ and $E3$ transitions, the simple patterns exhibited by these data are well reproduced by a binary cluster model. [S0556-2813(99)07902-9]

PACS number(s): 21.60.Gx, 23.20.Js, 27.90.+b

There has been a recent accumulation of data on $E1$, $E2$, and $E3$ transitions between states belonging to the lowest positive and negative parity bands of nuclei in the actinide region [1–6]. These data, involving the decays of levels up to quite large J^{π}, exhibit a simple overall behavior which, in the case of $E2$ and $E3$ transitions, can be reproduced using a binary cluster model whose principal properties are summarized below.

We describe each of these nuclei as an appropriate core-cluster pair, interacting through a potential $V(r)=V_N(r)+V_C(r)$, with r the core-cluster separation, and $V_N(r)$ and $V_C(r)$ the nuclear and Coulomb components of $V(r)$, respectively. $V_N(r)$ is assumed parity dependent, and for positive parity we use a prescription which results in good fits to data on the energy levels and exotic decays of nuclei in this mass region [7–9], i.e.,

$$V_N(r)=-V_0^{+}A_c\left[\frac{x}{1+\exp[(r-R^{+})/a]}+\frac{1-x}{(1+\exp[(r-R^{+})/3a])^3}\right]\ \mathrm{MeV}, \tag{1}$$

where A_c is the cluster mass, $V_0^{+}=53.9$ MeV, $a=0.73$ fm, and $x=0.36$. The Coulomb potential $V_C(r)$ is taken to be that arising from a uniformly charged spherical core of the same radius, R^{+}, as $V_N(r)$. The radius R^{+} is chosen so as to optimize the overall fit to the energies in the ground-state band [9].

We choose clusters of ^{14}C, ^{20}O, ^{24}Ne, ^{28}Mg, and ^{32}Si to model the properties of selected isotopes of Ra, Th, U, Pu, and Cm, respectively, in line with previous applications. These choices are consistent with the observed exotic emissions of these nuclei, although in some cases exotic decay has not yet been observed, and in others more than one type of heavy-ion is emitted [10]. In addition, these choices can be justified to some extent *a posteriori* since, as we shall see later, the cluster charge is largely responsible for the calculated electromagnetic transition rates, and different choices of cluster charge lead to predictions of $B(E2)$ strengths (say) which are incompatible with the measured values. [For highly asymmetric mass partitions such as we deal with here, the $B(E\lambda)$ strengths, of multipolarity λ, are almost proportional to the cluster charge raised to the power λ.] Our simple prescription leads to satisfactory results, and there is as yet no need to refine the choice of cluster in the model. Nevertheless, it is possible that a number of cluster types contribute in some cases [9], and our prescription corresponds to *effective* values of cluster mass and charge. For example, there are grounds for proposing that, in addition to ^{212}Pb$+^{20}$O, ^{232}Th could be described as ^{210}Pb$+^{22}$O or ^{206}Hg$+^{26}$Ne. In fact, a superposition of such configurations is probably necessary to describe this nucleus fully, but at the moment, the available data have large error bars, and do not compel such a refinement. We, therefore, retain the simpler model employing a single cluster.

Solving the Schrödinger equation for the core-cluster relative motion then yields bands of states, each characterized by its value of the global quantum number $G=2n+L$, with n the number of nodes and L the angular momentum of a state of the band. Positive parity bands require $G=G^{+}$ even, and for the ground-state bands we set $G^{+}=5A_c$, consistent with the requirements of the Pauli principle, and with earlier work [7–9]. We thus obtain a $J^{\pi}=0^{+},2^{+},4^{+},\ldots,G^{+}$ ground-state band for each nucleus. We then use a similar procedure, with $V_0^{-}=0.965V_0^{+}$ and $G^{-}=G^{+}+1$, to generate the lowest $J^{\pi}=1^{-},3^{-},5^{-},\ldots$ negative parity band, and optimize its position by a suitable choice of the radius R^{-} [7–9].

The choice of the relative motion value G is guided by the Wildermuth condition [11] and the spherical shell model. Protons and neutrons outside a ^{208}Pb core must have at least five and six quanta, respectively. A ground state (sd)-shell cluster nucleus consisting of $(0s)^4(0p)^{12}(1s0d)^{(A_c-16)}$ nucleons requires $2A_c-20$ quanta for its construction [and ^{14}C, the only non-(sd)-shell cluster we consider, requires 10 quanta]. Hence, for a general (sd)-shell cluster we need *at least* $(Z_c\times 5)+([A_c-Z_c]\times 6)-[2A_c-20])=(4A_c-Z_c+20)$ quanta for the cluster-core relative motion. This value should not be regarded as more than a reasonable guess, since for the heavy systems of interest here the core and cluster have very different masses (and hence oscillator constants), and the spin-orbit force strongly shifts single-particle energies from a harmonic-oscillator spectrum as well.

Previous experience with α particles [12] has shown that the value of G and the potential parameters cannot be deter-

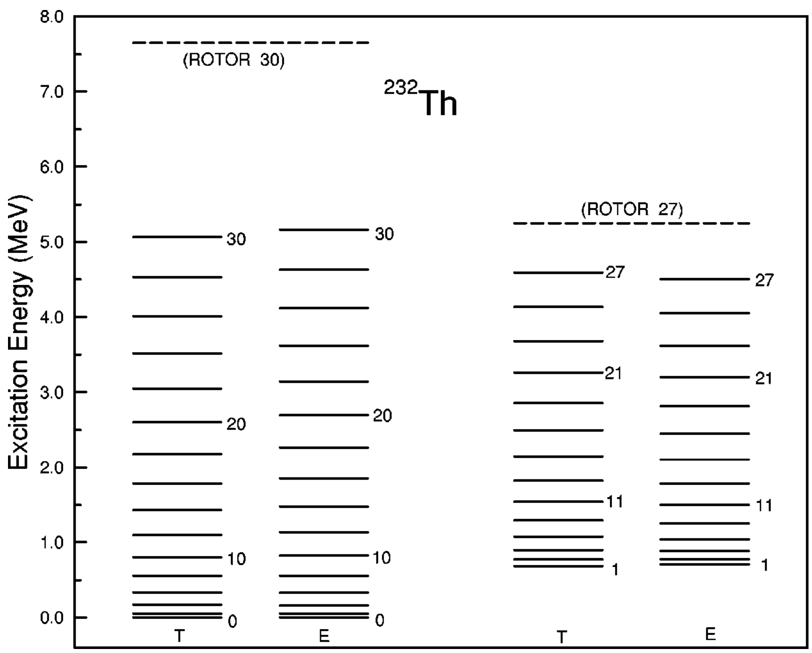

FIG. 1. Theoretical (T) and experimental (E) energy levels of the ground state $J^{\pi}=0^{+},2^{+},4^{+},\ldots$ and excited $J^{\pi}=1^{-},3^{-},5^{-},\ldots$ bands of ^{232}Th. A rigid rotor prediction, based on the 0^{+}–2^{+} energy difference, for the energy of the 30^{+} state is 7.652 MeV. Similarly, based on the 3^{-}–1^{-} separation, the rigid rotor predicts the 27^{-} state at 5.250 MeV.

mined separately in a unique way. Rather, within fairly wide limits, the values fall into families which describe the half-lives, spectra, and electromagnetic transition rates more or less equally well. This outcome is repeated for exotic clusters. One family of acceptable parameters has been found in which the potential depth and the G-value scale in direct proportion to the cluster mass [13]. In view of the compatibility of this behavior with expectations from folding models of the the cluster-core potential depth, and our wish to avoid the introduction of unnecessary free parametrization in the present calculations, we here adopt a formulation unchanged from our previous work [7–9]. Other G values could certainly be chosen instead, but would entail small compensatory adjustments of the potential parameters. Our simple formula $G=5A_c$ avoids such changes, is clearly compatible with the Wildermuth restriction for the cases of interest here, and works very well also in all other actinides examined so far.

We apply the model to ^{226}Ra, ^{232}Th, ^{234,236,238}U, and ^{248}Cm, with these nuclei treated as a Pb core plus a ^{14}C, ^{20}O, ^{24}Ne, and ^{32}Si cluster, respectively. Figure 1 shows the excellent agreement between theory and experiment obtained for the excitation energies of states belonging to the lowest 0^{+} and 0^{-} bands of ^{232}Th, using $R^{+}=6.715$ fm and $R^{-}=6.877$ fm. Similarly good fits for the remaining nuclei require at most small changes in the values of the core-cluster potential parameters defined above [9]. Of interest also is that the large $B(E2\downarrow;2^{+}\rightarrow 0^{+})$ values observed in this region, and their systematic increase with atomic number for the sequence Ra→Th→U→Pu→Cm, are easily understood in terms of the cluster model [9]. A further, and very important, characteristic of the model is shown in Fig. 2 where the radial wave functions χ_L^{+} and χ_L^{-} of states belonging to the 0^{+} and 0^{-} bands of ^{232}Th are compared. We see that the χ_L within a band are all very similar in the important surface region, implying a common intrinsic state for each band [14].

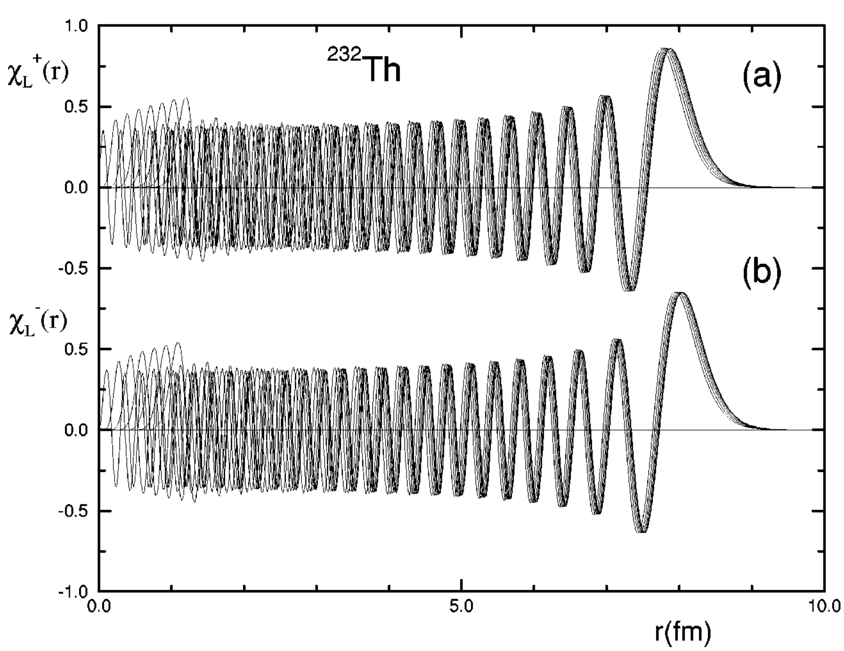

FIG. 2. Dependence of radial wave functions on cluster-core separation r (fm), for (a) positive parity with $L=0(4)28$ and (b) negative parity with $L=1(4)25$.

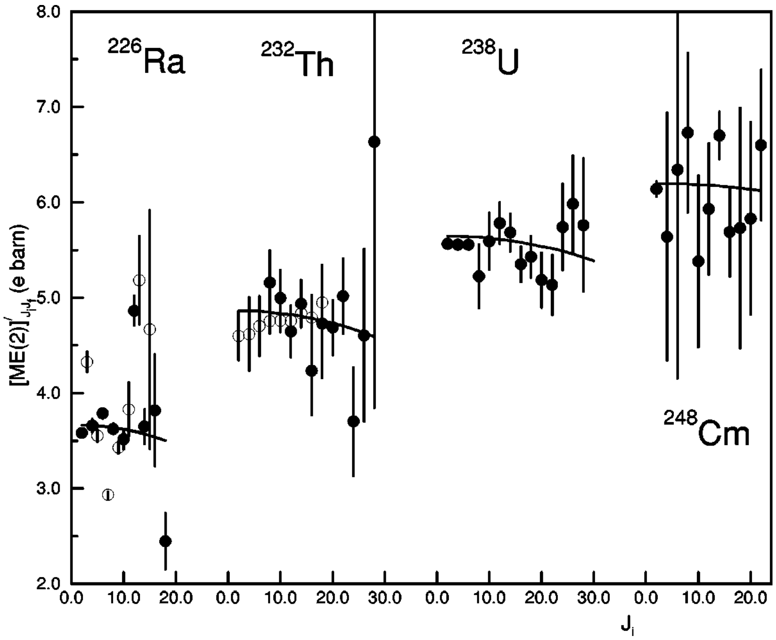

FIG. 3. Calculated (solid lines) and measured (circles with error bars) values of $[ME(2)]'_{J_iJ_f}$ (e barn) as functions of J_i. Data for ^{226}Ra are from Ref. [2] and include both positive (full circles) and negative (open circles) parity states. Data for all other nuclei are for positive parity states only. Sources are; ^{232}Th Ref. [20] (open circles), Ref. [3] (full circles), ^{238}U Ref. [4] and ^{248}Cm Ref. [6].

We summarize the above by noting that for a typical nucleus in the actinide region our binary cluster model results in a $J^{\pi}=0^+,2^+,4^+,\ldots$ ground-state band, based on a common intrinsic state, with energy spacings and strongly collective in-band $E2$ transitions closely matching observations, and similarly for an excited $J^{\pi}=1^-,3^-,5^-,\ldots$ band. The model is then able to generate additional structure more usually associated with the conventional rotational model [15]. This has been explicitly demonstrated in calculations of the spectra of ^{223}Ra and ^{223}Ac [16,17], modeled as ^{208}Pb $+{}^{14}$C$+n$ and ^{208}Pb$+{}^{14}$C $+p$, respectively, which reproduced the properties of the parity doublet K-bands of these nuclei.

It is also clear from Fig. 2 that the model gives rise to approximately constant radial matrix elements $\langle\chi_f|r^{\lambda}|\chi_i\rangle$, whenever χ_i and χ_f are radial wave functions belonging to the same band, and $\lambda=2,4,\ldots$. Similar remarks apply when χ_i and χ_f belong to bands of opposite parity, and $\lambda=1,3,\ldots$. These conclusions will be reinforced if, as suggested by microscopic calculations of α clustering in ^{212}Po [18], our model overestimates the amplitudes of the radial wave functions in the central region. A test of these conclusions is provided by electric transitions of multipolarity λ, for which the model yields reduced matrix elements of the form

$$[ME(\lambda)]_{J_iJ_f}=\langle J_f||ME(\lambda)||J_i\rangle=f(J_i,J_f,\lambda)\alpha_{\lambda}\langle r^{\lambda}\rangle, \tag{2}$$

with

$$f(J_i,J_f,\lambda)=\sqrt{\frac{(2J_i+1)(2J_f+1)}{4\pi}}\langle J_i0J_f0|\lambda 0\rangle \tag{3}$$

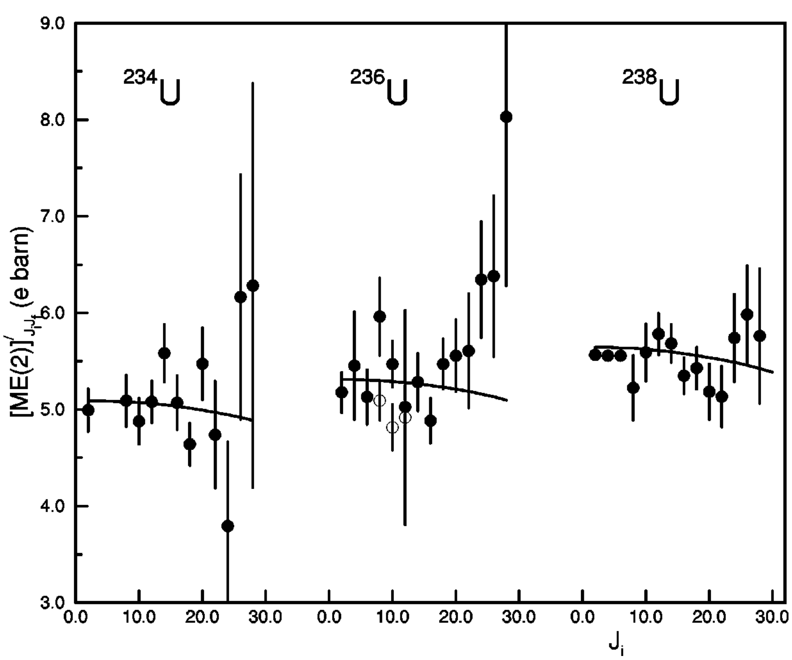

FIG. 4. Calculated (solid lines) and measured (circles with error bars) values of $[ME(2)]'_{J_iJ_f}$ (e barn) as functions of J_i. Data for ^{234}U are from Ref. [3], ^{236}U Ref. [21] (open circles), Ref. [3] (full circles), and ^{238}U Ref. [4].

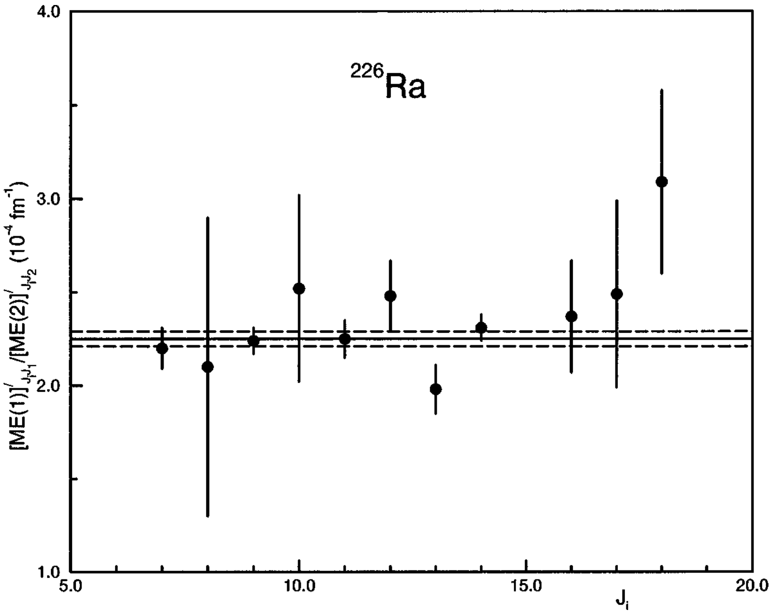

FIG. 5. Weighted mean values of $[ME(1)]'_{J_iJ_1}/[ME(2)]'_{J_iJ_2}$ and corresponding errors for each $J_i \geqslant 7$ in ^{226}Ra. Data are from Refs. [1], [2], [5]. The overall mean value and standard deviation deduced from the data, $(2.25 \pm 0.04) \times 10^{-4}$ fm^{-1}, are indicated by solid and broken horizontal lines, respectively.

and

$$\alpha_\lambda = \frac{Z_1 A_2^\lambda + (-1)^\lambda Z_2 A_1^\lambda}{(A_1 + A_2)^\lambda}. \tag{4}$$

Z_i and A_i are the charge and mass of cluster and core, respectively, and an effective charge ϵ can be introduced by substituting $Z_i \rightarrow Z_i + \epsilon A_i$. We remove the sign and explicit J dependence of the matrix elements by defining

$$[ME(\lambda)]'_{J_iJ_f} = |[ME(\lambda)]_{J_iJ_f}/f(J_i, J_f, \lambda)|. \tag{5}$$

Most of the data [1–6] involve in-band $\lambda = 2$ transitions. Figures 3 and 4 show that the model reproduces the essentially constant $[ME(2)]'_{J_iJ_f}$ within each band, as well as the observed jumps with atomic number. These jumps are the direct consequences of the increasing cluster charge, although some fine-tuning using the effective charge is required ($\epsilon = 0.33, 0.32, 0.21, 0.24, 0.29$, and 0.15 for ^{226}Ra, ^{232}Th, ^{234,236,238}U, and ^{248}Cm, respectively). We note that although these results could be reproduced by suitably parametrized rigid rotors, the latter would lead to poor fits to the excitation energies, which depart markedly from a $J(J+1)$ pattern as seen in Fig. 1. Again, the cluster model $[ME(2)]'_{J_iJ_f}$ for a given nucleus already show some variation for the higher J_i, unlike the case for the intrinsic quadrupole moment Q_0 of a rigid rotor, and it would be interesting to have data for yet larger spins.

Measurements of cross band $E1$ and $E3$ transitions have also been reported. Data on $E1$ transitions in the form of $E1/E2$ intensity ratios [1,2,5] are principally from the work of Ackermann *et al.* [5], who deduce $|D_0/Q_0|$ values for several transitions within each of the nuclei ^{226}Ra, ^{224,226,228,232}Th, and ^{230,232}U. Their conclusion is that, except possibly for ^{224}Th, these ratios show no depen-

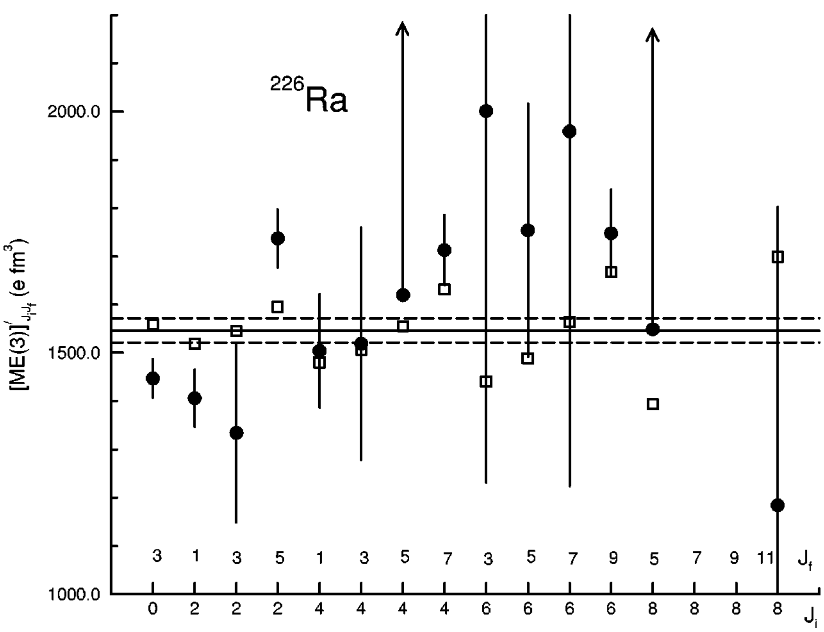

FIG. 6. Calculated (open squares) and measured values (full circles with error bars) of $[ME(3)]'_{J_iJ_f}$ (e fm^3) for ^{226}Ra as functions of J_i and J_f. Data are from Wollersheim *et al.* [2]. The overall mean value and standard deviation deduced from the data, 1546 ± 25 e fm^3, are indicated by solid and broken horizontal lines, respectively.

dence on rotational frequency. For ^{226}Ra, there are a number of independent determinations of the $E1/E2$ intensity ratios for initial states with $J_i \geqslant 7$. These result in the approximately constant $[ME(1)]'_{J_iJ_1}/[ME(2)]'_{J_iJ_2}$ ratios shown in Fig. 5. One experiment [2] yields sharply lower values of this ratio for $J_i < 7$, possibly indicating a similar behavior to that found for $E1$ transitions in some lighter nuclei [22]. We do not make detailed comparison with calculation here, since dipole transitions are not reliably deterimined in our model, with the charge factor α_1 of Eq. (4) involving the residue of strong cancellations between core and cluster charge/mass ratios [7,16].

For ^{226}Ra we can also extract $[ME(3)]'_{J_iJ_f}$ from data on $E3$ transitions between the 0^+ and 0^- bands [2], and in Fig. 6 we compare the results with the corresponding model predictions. The observed $[ME(3)]'_{J_iJ_f}$ are approximately constant within rather large experimental errors, and are reproduced by the model using a somewhat larger effective charge $\epsilon = 0.48$ than the $\epsilon = 0.33$ required to fit the $[ME(2)]'_{J_iJ_f}$ for the same nucleus. We note, however, that the value of $[ME(3)]'_{30}$ deduced by Wollersheim *et al.* [2] is 50% larger than the corresponding quantity quoted by Spear [19].

In conclusion, a remarkable characteristic of our binary cluster model is that it gives rise to similar radial wave functions for states belonging to the lowest 0^+ and 0^- bands of nuclei in the actinide region. One consequence of this is that the radial matrix elements of the type $\langle r^\lambda \rangle$ for either the in-band E2 or the cross-band $E3$ transitions within a given nucleus are predicted to be approximately constant, and the model reproduces well the simple patterns exhibited by the available data.

A.C.M. and S.M.P would like to thank the U.K. Engineering and Physical Science Research Council (EPSRC) for financial support. S.M.P. would also like to thank the S.A. Foundation for Research, and the University of Cape Town, for financial support.

[1] J.F.C. Cocks, P.A. Butler, K.J. Cann, P.T. Greenlees, G.D. Jones, S. Asztalos, P. Bhattacharyya, R. Broda, R.M. Clark, M.A. Deleplanque, R.M. Diamond, P. Fallon, B. Fornal, P.M. Jones, R. Julin, T. Lauritsen, I.Y. Lee, A.O. Macchiavelli, R.W. MacLeod, J.F. Smith, F.S. Stephens, and C.T. Zhang, Phys. Rev. Lett. **78**, 2920 (1997).

[2] H.J. Wollersheim, H. Emling, H. Grein, R. Kulessa, R.S. Simon, C. Fleischmann, J. de Boer, E. Hauber, C. Lauterbach, C. Schandera, P.A. Butler, and T. Czosnyka, Nucl. Phys. **A556**, 261 (1993).

[3] H. Ower, Th.W. Elze, J. Idzko, K. Stelzer, E. Grosse, H. Emling, P. Fuchs, D. Schwalm, H.J. Wollersheim, N. Kaffrell, and N. Trautmann, Nucl. Phys. **A388**, 421 (1982).

[4] E. Grosse, A. Bałandal, H. Emling, F. Folkmann, P. Fuchs, R.B. Piercey, D. Schwalm, R.S. Simon, H.J. Wollersheim, D. Evers, and H. Ower, Phys. Scr. **24**, 337 (1981).

[5] B. Ackermann, H. Baltzer, C. Ensel, K. Freitag, V. Grafen, C. Günther, P. Herzog, J. Manns, M. Marten-Tölle, U. Müller, J. Prinz, I. Romanski, R. Tölle, J. deBoer, N. Gollwitzer, and H.J. Maier, Nucl. Phys. **A559**, 61 (1993).

[6] T. Czosnyka, D. Cline, L. Hasselgren, C.Y. Wu, R.M. Diamond, H. Kluge, C. Roulet, E.K. Hulet, R.W. Lougheed, and C. Baktash, Nucl. Phys. **A458**, 123 (1986).

[7] B. Buck, A.C. Merchant, and S.M. Perez, Nucl. Phys. **A617**, 195 (1997).

[8] B. Buck, A.C. Merchant, and S.M. Perez, Nucl. Phys. **A625**, 554 (1997).

[9] B. Buck, A.C. Merchant, and S.M. Perez, Phys. Rev. C **58**, 2049 (1998).

[10] B. Buck, A.C. Merchant, S.M. Perez, and P. Tripe, J. Phys. G **20**, 351 (1994).

[11] B. Buck, H. Friedrich, and C. Wheatley, Nucl. Phys. **A275**, 246 (1977).

[12] B. Buck, A.C. Merchant, and S.M. Perez, Phys. Rev. C **45**, 2247 (1992).

[13] B. Buck, A.C. Merchant, and S.M. Perez, Nucl. Phys. **A614**, 129 (1997).

[14] B. Buck, A.C. Merchant, and S.M. Perez, Phys. Rev. C **57**, R2095 (1998).

[15] D.M. Brink, B. Buck, R. Huby, M.A. Nagarajan, and N. Rowley, J. Phys. G **13**, 629 (1987).

[16] B. Buck, A.C. Merchant, and S.M. Perez, Nucl. Phys. **A634**, 15 (1998).

[17] B. Buck, A.C. Merchant, and S.M. Perez, Phys. Rev. C **58**, 2990 (1998).

[18] K. Varga, R.G. Lovas, and R.J. Liotta, Phys. Rev. Lett. **69**, 37 (1992); Nucl. Phys. **A550**, 421 (1992).

[19] R.H. Spear, At. Data Nucl. Data Tables **42**, 55 (1989).

[20] M.W. Guidry, P.A. Butler, P. Colombani, I.Y. Lee, D. Ward, R.M. Diamond, F.S. Stephens, E. Eichler, N.R. Johnson, and R. Sturm, Nucl. Phys. **A266**, 228 (1976).

[21] M.W. Guidry, R.J. Sturm, N.R. Johnson, E. Eichler, G.D. O'Kelley, N.C. Singhal, and R.O. Sayer, Phys. Rev. C **13**, 1164 (1976).

[22] E. Garrote, J.L. Egido, and L.M. Robledo, Phys. Rev. Lett. **80**, 4398 (1998).